



Observation of coherent hybrid reflection with synchrotron radiation

S. L. Morelhão, L. H. Avanci, M. A. Hayashi, L. P. Cardoso, and S. P. Collins

Citation: [Applied Physics Letters](#) **73**, 2194 (1998); doi: 10.1063/1.122420

View online: <http://dx.doi.org/10.1063/1.122420>

View Table of Contents: <http://scitation.aip.org/content/aip/journal/apl/73/15?ver=pdfcov>

Published by the [AIP Publishing](#)

Articles you may be interested in

[High-resolution X-ray diffraction analysis of \$\text{Al}_x\text{Ga}_{1-x}\text{N}/\text{In}_x\text{Ga}_{1-x}\text{N}/\text{GaN}\$ on sapphire multilayer structures: Theoretical, simulations, and experimental observations](#)

[J. Appl. Phys.](#) **115**, 174507 (2014); 10.1063/1.4875382

[In situ X-ray investigation of changing barrier growth temperatures on InGaN single quantum wells in metal-organic vapor phase epitaxy](#)

[J. Appl. Phys.](#) **115**, 094906 (2014); 10.1063/1.4867640

[Structural and electrical characteristics of \$\text{Ga}_2\text{O}_3\$ \(\$\text{Gd}_2\text{O}_3\$ \) GaAs under high temperature annealing](#)

[J. Appl. Phys.](#) **100**, 104502 (2006); 10.1063/1.2386946

[Mechanical behavior of thin buffer layers in InAs/GaAs\(111\) A heteroepitaxy](#)

[Appl. Phys. Lett.](#) **76**, 3017 (2000); 10.1063/1.126564

[Molecular beam epitaxial growth of InAs/AlGaAsSb deep quantum well structures on GaAs substrates](#)

[J. Vac. Sci. Technol. B](#) **16**, 2644 (1998); 10.1116/1.590249



AIP | Journal of Applied Physics

Journal of Applied Physics is pleased to announce **André Anders** as its new Editor-in-Chief

Observation of coherent hybrid reflection with synchrotron radiation

S. L. Morelhão^{a)}

Instituto de Física, Universidade de São Paulo, CP 66318, 05315-970 São Paulo, SP, Brazil

L. H. Avanci, M. A. Hayashi, and L. P. Cardoso

Instituto de Física Gleb Wataghin, UNICAMP, CP6165, 13083-970 Campinas, SP, Brazil

S. P. Collins

CCLRC Daresbury Laboratory, Warrington WA4 4AD, United Kingdom

(Received 17 December 1997; accepted for publication 14 August 1998)

High resolution synchrotron radiation has been used to investigate the occurrence of coherent hybrid reflections (CHR) in the $\text{In}_{0.49}\text{Ga}_{0.51}\text{P}/\text{GaAs}(001)$ structure. Several ϕ scans at the 002 layer reflection were carried out. The scanned ϕ intervals are correlated by the [001] axis symmetry and should present the same pattern. A break in the symmetry is observed due to constructive/destructive interference of the hybrid amplitudes with the amplitude from the 002 layer reflection. The effects of substrate miscut and interface distance are taken into account to explain the observed patterns. The application of CHR as a high sensitive tool to analyze epitaxial growth is discussed.

© 1998 American Institute of Physics. [S0003-6951(98)03841-8]

In research for understanding a physical phenomenon, very often a new technique for materials analysis comes out, as in the case of the x-ray multiple diffraction (MD) phenomenon.¹ Besides its most important applications, a solution for the ‘‘phase problem’’,^{2,3} the investigation of this phenomenon has generated several procedures to analyze epitaxial structure⁴ and semiconductor surfaces.^{5,6}

MD arises when two or more reciprocal lattice points (r.l.p.) are touching the Ewald sphere. In order to systematically generate MD, the crystal is first aligned by a ω rotation for a symmetric Bragg reflection, the primary reflection 01 . The ϕ rotation of the crystal around the reciprocal vector of the primary reflection, \mathbf{H}_{01} , brings additional reflections, secondary reflections $0i$ ($i=2,3,\dots$), to simultaneously diffract the incident beam. Bragg or Laue-types of secondary reflection specify the secondary beam direction above or below the crystal surface, respectively. The interactions among the diffracted beams inside the crystal modify the primary intensity that is monitored in a ϕ scan. The coupling reflections are responsible for such interactions, and their reciprocal lattice vectors are given by $\mathbf{H}_{ij}=\mathbf{H}_{0j}-\mathbf{H}_{0i}$.

Hybrid reflections⁴ occur in epitaxial structures close to MD conditions.¹ They are different sequences of reflections inside the layer/substrate structure where the secondary and coupling reflections are not in the same lattice. Hereafter, subscript L or S will be used to indicate reflection in the layer or substrate lattice, respectively. In the ϕ scan of the 01_L primary reflection, 02_L (Laue) and 03_L (Bragg) are the secondary reflections of a typical four-beam diffraction in the layer. In Fig. 1 are illustrated the two types of hybrid reflections, labeled as LS and SL,⁴ that occur near this four-beam diffraction. The hybrids are specified by their sequence of reflections, 03_S+31_L [SL hybrid, Fig. 1(a)] and 02_L+21_S [LS hybrid, Fig. 1(b)].

The feature about hybrid reflection that we would like to

present here is the interference of the wave fields from hybrid reflections with the primary reflection. If they can interfere, it means the coherence of the x-rays is preserved along the hybrid path (sequence of reflections). So, we call them coherent hybrid reflection (CHR). All cases of hybrids investigated in the past were incoherent since they had always been observed as a positive contribution to the primary intensity, i.e., as superposition of intensities.

High resolution ϕ scans were carried out in the station 16.3 at Daresbury Synchrotron Radiation Laboratory. The ω and ϕ axes of the six-axis diffractometer allow us to perform scans with minimum step size of 0.0004° and accuracy less than 0.008° . The beamline monochromator provides photons in a wavelength (λ) of $1.48676(5)$ Å. The procedure to determine λ , based on the SL hybrid occurrence, is described later. Cross-slit screen also limits the divergence of the beam to about 4 arcsec in both ω and ϕ scans.

The sample used here is a $\text{In}_x\text{Ga}_{1-x}\text{P}$ layer grown on top of $\text{GaAs}(001)$ substrate by chemical beam epitaxy (CBE). It was characterized by four ω scans of the 002 reflection performed at $\phi=0^\circ, 90^\circ, 180^\circ$, and 270° . They all are identical to the one shown in Fig. 2 (for $\phi=0^\circ$). Then, no relative tilt between the lattices exists. From data fitting,⁷ the thickness and the perpendicular lattice parameter of the layer are 470 nm and 5.6568 Å ($x=0.49$), respectively. A miscut of $0.6(\pm 0.1)^\circ$ in the $[110]$ direction was measured in the sample by reflection of a laser beam.

By choosing the 002 layer reflection as the 01_L primary

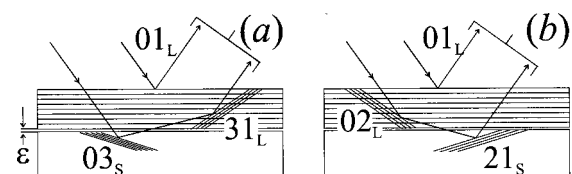


FIG. 1. Planar scheme of the SL and LS hybrid reflections, (a) 03_S+31_L and (b) 02_L+21_S respectively. These hybrids occur in the ϕ scan of the 01_L primary reflection.

^{a)}Electronic mail: morelhao@if.usp.br

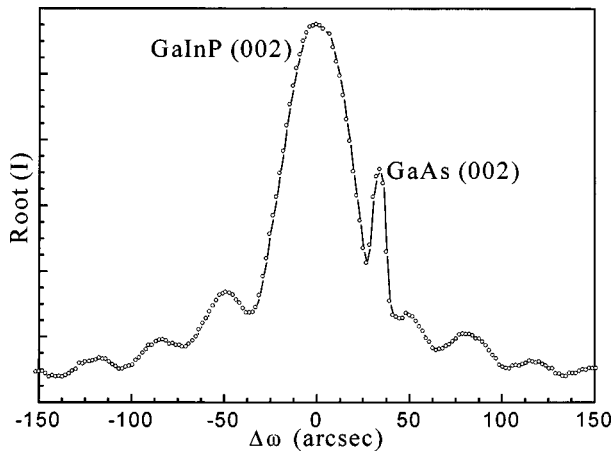


FIG. 2. Rocking curve (ω scan) of the 002 reflection in $\text{In}_{0.49}\text{Ga}_{0.51}\text{P}/\text{GaAs}$ (001) epitaxial structure. Synchrotron radiation of photons at $\lambda=1.48676$ Å.

reflection, three four-beam diffractions with secondary reflections $\bar{1}\bar{1}\bar{1}_L/\bar{1}\bar{1}3_L$, $200_L/202_L$ and $3\bar{1}\bar{1}_L/313_L$ occur in a short interval ($<1^\circ$) of the ϕ scan, around $\phi=29^\circ$. The $[110]$ direction is taken as the reference position¹ ($\phi=0$), and the notation $02_L/03_L$ (Laue/Bragg) has been employed. The pattern observed in this interval repeats over the ϕ scan obeying the mirror symmetry of the $[001]$ zone axis, therefore, at intervals around $\phi=29^\circ$, 61° , 119° , 151° , ..., 331° . Also, it has been defined a notation, such as $\{hk\}_L/\{hk\}_L$, in order to specify the families of four-beam diffractions that appear in positions related only by the symmetry of the zone axis.

We have measured three families of four-beam diffractions, $\{\bar{1}\bar{1}\}_L/\{\bar{1}\bar{1}\}_L$, $\{20\}_L/\{20\}_L$ and $\{3\bar{1}\}_L/\{3\bar{1}\}_L$, in the intervals around $\phi=29^\circ$ (scan A), 61° (scan B), 119° (scan C), and 151° (scan D). For comparison purposes, these ϕ scans are shown in Fig. 3 on the same interval as the first one. The positions of the $\{20\}_L/\{20\}_L$ peaks, well determined by their sharp asymmetric profiles,³ were used to correct the ϕ scale from zero position error. After that, each

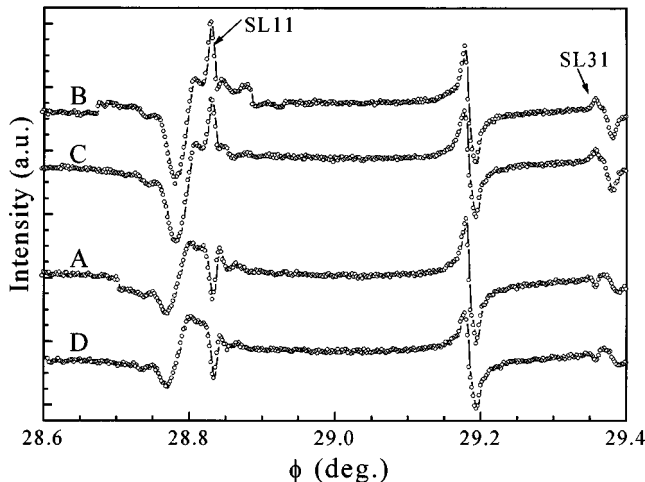


FIG. 3. Several ϕ scans performed at the 002 layer diffraction peak (Fig. 2). They were measured in different ϕ intervals: $[28.6, 29.4]$ (scan A), $[60.6, 61.4]$ (scan B), $[118.6, 119.4]$ (scan C), and $[150.6, 151.4]$ (scan D). For comparison purposes, they are shown in the same interval of the scan A. The arrows indicate the position of the hybrid reflections.

TABLE I. Experimental ϕ position of the SL hybrids in the ϕ scans of Fig. 3 and the β , ω and λ values determined from these positions. Angular values in degrees and λ in Å.

SL Hybrid	scan	ϕ^{exp} ± 0.0020	β ± 0.0020	ω ± 0.0031	λ ± 0.00005	$\Omega(\phi)$ ± 0.01
$\bar{1}\bar{1}3_S + \bar{1}\bar{1}\bar{1}_L$ $3\bar{1}3_S + 3\bar{1}\bar{1}_L$	A	28.8258	61.1742	15.2375	1.48672	5.629
		29.3527	55.9178			5.657
$113_S + \bar{1}\bar{1}\bar{1}_L$ $\bar{3}\bar{1}3_S + 3\bar{1}\bar{1}_L$	B	61.1768	61.1768	15.2404	1.48681	5.603
		60.6477	55.9174			5.574
$\bar{1}\bar{1}3_S + 11\bar{1}_L$ $\bar{1}\bar{3}3_S + \bar{1}\bar{3}\bar{1}_L$	C	118.8248	61.1752	15.2385	1.48675	5.603
		119.3527	55.9178			5.574
$\bar{1}\bar{1}3_S + \bar{1}\bar{1}\bar{1}_L$ $\bar{1}\bar{3}3_S + \bar{1}\bar{3}\bar{1}_L$	D	151.1726	61.1726	15.2366	1.48671	5.629
		150.6477	55.9174			5.657

interval was projected to the interval around $\phi=29^\circ=90^\circ-61^\circ=119^\circ-90^\circ=180^\circ-151^\circ$.

Two families of SL hybrid reflections are clearly visible in the scans, $\{\bar{1}\bar{1}\}_L/\{3\bar{1}\}_L$ and $\{3\bar{1}\}_L/\{\bar{1}\bar{1}\}_L$, labeled SL11 and SL31, respectively. They are shown by arrows in the figure, and their experimental positions are given in Table I. The layer four-beam diffractions, $\{\bar{1}\bar{1}\}_L/\{\bar{1}\bar{1}\}_L$, $\{20\}_L/\{20\}_L$ and $\{3\bar{1}\}_L/\{3\bar{1}\}_L$, are seen at $\phi \approx 28.78^\circ$, $\phi \approx 29.16^\circ$, and $\phi \approx 29.38^\circ$, respectively. The most interesting feature in these scans is the break in the mirror symmetry of the zone axis regarding the mirrors at 45° and 135° . Such symmetry break is characterized by either the SL hybrids appearing as peaks or as dips and the different changes in the $\{\bar{1}\bar{1}\}_L/\{\bar{1}\bar{1}\}_L$ and $\{3\bar{1}\}_L/\{3\bar{1}\}_L$ profiles due to the LS hybrids. In spite of this fact, and before we get into it, the SL hybrids will be used to determine the wavelength, λ , and also to check the incidence angle, ω , in which each ϕ scan was performed. In general, variation in the ω angle during a long ϕ rotation occurs due to small misalignments between \mathbf{H}_{01} and the ϕ axis.

The SL hybrid appears when the 03_S r.l.p. crosses the Ewald sphere. Its position depends on ω , λ , and a_0 (the substrate lattice parameter). It can be calculated by the equations⁴ $\phi = \alpha \pm \beta$ and $\cos \beta = [\lambda/2a_0(h^2 + k^2 + l^2) - l \sin \omega] / \sqrt{h^2 + k^2} \cos \omega$ where 2β is the angle between the two ϕ positions in which the 03_S r.l.p. crosses the Ewald sphere (out/in and in/out positions). The term α stands for the angle between the $[110]$ reference direction and the projection of \mathbf{H}_{03_S} into the $[001]$ zone. The term hkl is the Miller index of the 03_S reflection.

These equations are used here to determine both ω and λ values from the measurements of two different families of SL hybrid reflections (Table I). These values from each ϕ scan in Fig. 3 are also shown in Table I. They were determined by plotting $\Delta\beta = \beta^{\text{calc}} - \beta^{\text{exp}}$ vs ω for the SL11 and SL31 hybrids. The experimental ω value is given by the intersection of the two plots, and λ is adjusted in order to set the intersection to $\Delta\beta=0$. These results show that the ϕ scans were performed at near the maximum of the 002 layer peak ($\omega=15.238^\circ$, full width at half maximum (FWHM) = 34.7 arcsec) with an accuracy better than 0.0033° (12 arcsec). The experimental wavelength (average from the scans) has been determined by this procedure as $1.48676(5)$ Å.

The proof that the hybrid reflections observed in the ϕ scans (Fig. 3) are CHR is provided by the symmetry breaks mentioned above. SL hybrids appearing as peaks or as dips demonstrate the constructive or destructive interference of the x-ray wave field (amplitude) scattered by the hybrid reflections with the wave field from the 01_L primary reflection. The changes in the profiles of the layer four-beam diffractions are also due to the interference with the wave field from hybrid reflections, LS hybrid in these cases.

The ω value is practically the same for all scans. Since it is constant, the ϕ rotation should not affect the path length in samples with an in-plane isomorphism. Therefore, it allows us to assume that some morphologic difference must exist between the in-plane $[110]$ and $[\bar{1}10]$ directions, as, for instance, the miscut of the substrate.

The function $\delta(\phi) = \delta_0 \sin(\phi)$ will be used to express the projection of the miscut in the primary incidence plane. By taking ϵ as the interface distance,⁸ the interfacial separation between the last monolayer of atoms in the substrate and the first diffracting one in the epilayer. The assigned phase shift for a hybrid reflection is the following: $\varphi = 2\pi(1/\sin \delta_1 + 1/\sin \delta_2)\epsilon/\lambda = 2\pi\Omega(\phi)\epsilon/\lambda$ where δ_1 and δ_2 are the angles in which the beams cross the interface in the hybrid path. For the SL hybrids, $\delta_1 = \omega_1 + \delta(\phi)$, $\delta_2 = \omega_2 + \delta(\phi + \pi \pm \phi')$, $\omega_1 = \omega (= 15.238^\circ)$, and $\omega_2 = \sin^{-1}(\lambda/a_0 - \sin \omega_1) (= 31.744^\circ)$. The in-plane direction of the secondary beam is given by $\phi + \pi \pm \phi'$. The Ewald construction allows to calculate ϕ' as $\tan^{-1}[\lambda\sqrt{h^2+k^2} \sin \beta / (a_0 \cos \omega - \lambda\sqrt{h^2+k^2} \cos \beta)]$, and then, ϕ' as 23.55° (SL11) and 56.22° (SL31). The + (or -) sign of ϕ' indicates an in/out (or out/in) movement of the 03_S r.l.p. with respect to the Ewald sphere.

The $\Omega(\phi)$ values for each measured SL hybrid are shown in Table I, calculated with $\omega = 15.238(3)^\circ$ and $\delta_0 = 0.6(1)^\circ$. These values are very well correlated with the hybrids appearing as peaks or as dips. For instance, the SL11 hybrids are peaks in the scans B and C since they have the same $\Omega(\phi)$ value. Note that only the symmetry of the mirror at $\phi = 90^\circ$ has been preserved by taking the miscut into account. Therefore, the symmetry break is due to the miscut. The question that still remains regards the fact that both SL11 and SL31 are peaks (or dips) in the scans B and C (or A and D). Is it a rule or just a coincidence?

The total intensity scattered by the sample is $I = |A_P + A_H(\phi)\exp(i\Phi + i\varphi)|^2$, where A_P and $A_H(\phi)$ are the amplitudes modulus from the primary and hybrid reflections, respectively. The triplet phase³ Φ takes into account the structure factor phases for the 01_L , 03_S and 31_L reflections. The behavior of the intensity maximum at each hybrid position can be understood by analyzing $\Delta I_{11} = (I_{BC} - I_{AD})_{SL11}$ and $\Delta I_{31} = (I_{BC} - I_{AD})_{SL31}$ as a function of ϵ/λ . The subscripts BC and AD indicate the hybrids appearing in the scans B or C and A or D. The oscillation periods of these ΔI functions are the same for both, and equal to $0.1780(3)$ (average of

$1/\Omega$). It is sensitive neither to small misalignment in ω nor to the miscut angle. The functions also have envelopes whose periods are different, $211(166)$ and $26(6)$ for ΔI_{11} and ΔI_{31} , respectively.

The oscillation periods tell us that the hybrid wave field changes from constructive to destructive interference with small variation in ϵ , of the order of 0.089λ ($\approx 0.13 \text{ \AA}$). The envelope periods describe the relationship between the SL11 and SL31 intensities. Since they are different, it is possible to observe SL11 and SL31 both as peaks, both as dips, and one as peak and the other as dip. For the analyzed sample, ϵ/λ value has to be in an interval where $\Delta I_{11} \gg \Delta I_{31} > 0$. The triplet phase Φ , different for each family of hybrid, does affect the position of such interval.

The absolute determination of the two major variables ϵ and Φ is a very complex problem because the actual modulus of the hybrid amplitudes, $A_H(\phi)$, are unknown. Even though, if $A_H(\phi)$ and ϵ could be measured or estimated, CHR can lead to a solution of the phase problem (determination of Φ) for epitaxial layers. Multiple diffraction procedures³ applied to solve the phase problem in epitaxial layers will always be affected by hybrid reflections.

In summary, the occurrence of coherent hybrid reflections (CHR) with synchrotron radiation has been reported. The long coherence length of the radiation is important to observe CHR since it has to be preserved along the hybrid path. The observed symmetry brake in the ϕ scans has been explained as a consequence of the substrate miscut. The CHR brings the prospect of a tool to high resolution analysis of semiconductor layer/substrate interfaces as well as of the in-plane morphology of the epitaxial growth. Very small changes ($\ll 0.1 \text{ \AA}$) in the interface distance can be observed by monitoring the hybrid intensity as a function of the illuminated area of the sample. The three-dimensional arrangement of the epitaxial growth structure is achieved by full ϕ rotation. Then, the isomorphism of the growth, with respect to the growth direction, can also be checked.

The authors wish to acknowledge the financial support of the Brazilian Agencies FAPESP, CNPq.

¹S. L. Chang, *Multiple Diffraction of X-Rays in Crystals*, Springer Series Solid-State Science, Vol. 50 (1984).

²B. Post, Phys. Rev. Lett. **39**, 760 (1977); Acta Crystallogr., Sect. A: Cryst. Phys., Diffraction, Theor. Gen. Crystallogr. **35**, 17 (1979).

³E. Weckert and K. Hummer, Acta Crystallogr., Sect. A: Found. Crystallogr. **A53**, 108 (1997).

⁴S. L. Morelhão and L. P. Cardoso, J. Appl. Phys. **73**, 4218 (1993); Solid State Commun. **88**, 465 (1993).

⁵S. L. Morelhão and L. P. Cardoso, J. Appl. Crystallogr. **29**, 446 (1996).

⁶M. A. Hayashi, S. L. Morelhão, L. H. Avanci, L. P. Cardoso, J. M. Sasaki, L. C. Kretly, and S. L. Chang, Appl. Phys. Lett. **71**, 2614 (1997).

⁷A. Pesek, P. Kastler, L. Palmetshofer, F. Hauzenberger, P. Juza, W. Faschinger, and K. Lischka, J. Phys. D **26**, A177 (1993).

⁸I. K. Robinson, R. T. Tung, and R. Feidenhans'l, Phys. Rev. B **38**, 3632 (1988).